Comparison of Airborne and Terrestrial Lidar Estimates of Seacliff Erosion in Southern California

Adam P. Young, M. J. Olsen, N. Driscoll, R.E. Flick, R. Gutierrez, R.T. Guza, E. Johnstone, and F. Kuester

Abstract

Seacliff changes evaluated using both terrestrial and airborne lidar are compared along a 400 m length of coast in Del Mar, California. The many large slides occurring during the rainy, six-month study period (September 2004 to April 2005) were captured by both systems, and the alongshore variation of cliff face volume changes estimated with the airborne and terrestrial systems are strongly correlated ($r^2 = 0.95$). However, relatively small changes in the cliff face are reliably detected only with the more accurate terrestrial lidar, and the total eroded volume estimated with the terrestrial system was 30 percent larger than the corresponding airborne estimate. Although relatively small cliff changes are not detected, the airborne system can rapidly survey long cliff lengths and provides coverage on the cliff top and beach at the cliff base.

Introduction

Terrestrial and airborne lidar (LIght Detection And Ranging) are rapidly emerging as the new standard for mapping and evaluating seacliff morphology (Adams and Chandler, 2002; Sallenger *et al.*, 2002; Collins, 2004; Collins and Sitar, 2004, 2008; Lim *et al.*, 2005; Rosser *et al.*, 2005; Brown *et al.*, 2006; Hapke and Reid, 2007; Miller *et al.*, 2007; Young, 2006; Young and Ashford, 2006a, 2006b, 2007, and 2008; Olsen *et al.*, 2008; Leyland and Darby, 2008). Although these relatively new technologies do not yet provide long-term observations comparable to conventional survey methods (topographic maps and aerial photographs), the accuracy and detail of lidar provides unprecedented resolution of short-term cliff change. This study compares quantified seacliff

changes in Del Mar, California (Figure 1 derived from both airborne and terrestrial lidar data collected in September 2004 and April 2005. Heavy rainfall during this six-month time period resulted in widespread cliff erosion and landsliding throughout the region. The differences between airborne and terrestrial lidar and their respective advantages and disadvantages applied to seacliff change analysis are also discussed.

Using Lidar to Map Seacliff Topography and Erosion

Terrestrial and airborne lidar are both capable of measuring cliff changes at sub-regional scales. However, at other spatial scales, each survey technique offers distinct advantages. Time requirements and limited beach access can complicate obtaining terrestrial lidar over long reaches. In addition to superior alongshore coverage, airborne lidar captures the cliff-top and crest, useful for estimating cliff-top retreat and detecting large or deep seated landslides, which extend beyond the cliff face. Conversely, the higher point density, accuracy, and mobility of the terrestrial lidar may be required to map specific landslides and small scale change. Further, terrestrial surveys capture over-vertical surfaces such as seacaves and notches (Figure 2). These features are important in slope failure analysis (Young and Ashford, 2008), and generally obscured during airborne surveying. As in other applications (e.g., mapping cityscapes; Iavarone and Vagners (2003) and Böhm and Haala (2005)), integrated terrestrial and airborne lidar provide comprehensive surface coverage (Figure 3).

Study Area

The study area covers 400 m of seacliffs in Del Mar, California (Figure 1). The seacliffs in the study area are cut into uplifted marine terraces and are approximately 18 m in height with a typical slope of 45°. Over-vertical features such as seacaves and wave cut notches which occasionally form in the region were not present during the study period. The cliffs are composed of the Del Mar Formation, an Eocene sedimentary deposit composed of sandy clay-stone interbedded with coarse grained sandstone (Kennedy, 1975). The cliff face is prone to weathering, desiccation, sheet erosion, rilling, and groundwater effects, while the cliff base is subject to wave action. Together, subaerial and marine erosional processes have resulted in long-term cliff

Adam P. Young, R.E. Flick, and R.T. Guza are with the Integrative Oceanography Division, Scripps Institution of Oceanography, University of California San Diego, 9500 Gilman Dr., La Jolla, CA, 92093 (adyoung@ucsd.edu).

M.J. Olsen is with the School of Civil and Construction Engineering, Oregon State University, 220 Owen Hall, Corvallis, OR 97331.

F. Kuester is with the Department of Structural Engineering, University of California San Diego, 9500 Gilman Dr., La Jolla, CA, 92093.

N. Driscoll and E. Johnstone are with the Geological Research Division, Scripps Institution of Oceanography, University of California San Diego, 9500 Gilman Dr., La Jolla, CA, 92093.

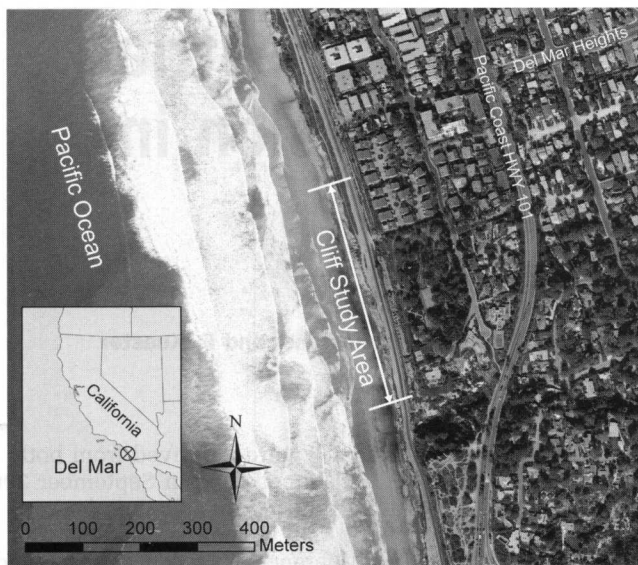R. Gutierrez is with the The University of Texas at Austin, 1 University Station, Austin, TX, 78712.

Figure 1. Del Mar study site located in southern California (Orthoimage from U.S. Geological Survey, EROS Data Center, Sioux Falls, South Dakota).
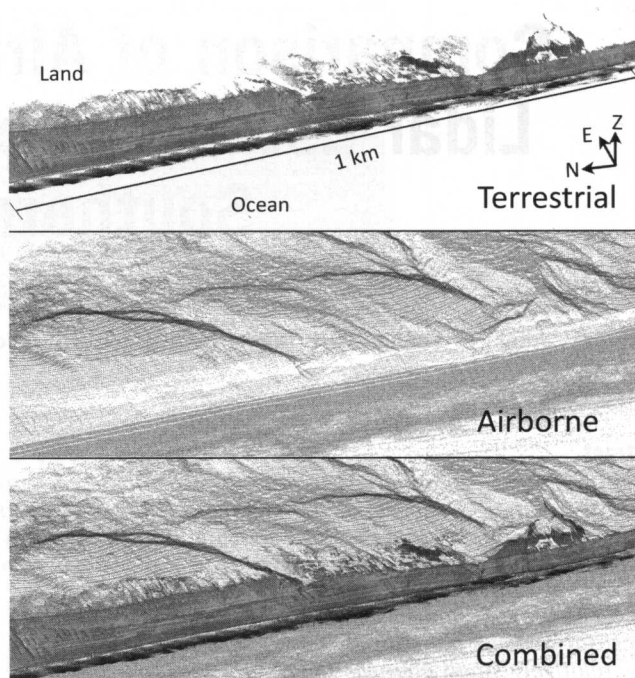

Figure 3. Comparison of terrestrial and airborne lidar point clouds on the tall (typically 80 m) seacliffs in Torrey Pines, California (located 5 km south of the Del Mar study area). Note, while the terrestrial lidar collects more data on the cliff face than the airborne lidar, the upper cliff and cliff top is obscured. Combining the terrestrial and airborne point clouds completes the spatial coverage and provides a comprehensive topographic cliff model.

top retreat rates estimated at 0.05 to 0.20 m/yr (Moore *et al.*, 1999; Benumof and Griggs, 1999; Young, 2006, Hapke and Reid, 2007). The San Diego, California, North County Transit District railroad, currently situated on the cliff top within a few meters of the cliff edge, has been threatened by cliff failures (Kuhn and Shepard, 1984).

Methods

Terrestrial lidar surveys were conducted with an I-Site 4400 laser scanner on 30 September 2004 and 07 April 2005. Each survey used seven overlapping scans setups, spaced at 50 to 80 m intervals alongshore and located 30 to 70 m from the cliff. The terrestrial lidar was filtered

with a maximum target distance of 150 m, an average point density of 70 points/m², and georeferenced using a differential Global Positional System (GPS) receiver mounted on top of the scanner and Maptek I-Site Studio
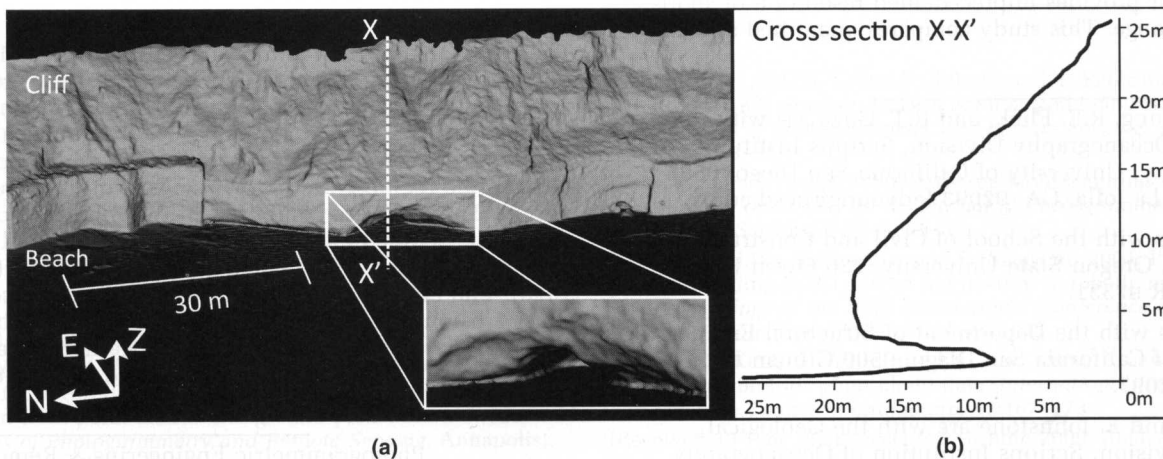

Figure 2. (a) Terrestrial lidar-based digital terrain model of seacliffs in Solana Beach (located 5 km north of the Del Mar study area) includes seacaves and wave cut notches, and (b) Cliff face horizontal location versus cliff face vertical location along the transect X-X'.

automated surface registration techniques (iterative least squares adjustment). The airborne lidar surveys were conducted on 28 September 2004, and 04 April 2005 with an Optech Airborne Laser Terrain Mapper ALTM 1225. Each airborne survey consisted of four passes with a 40° swath at an altitude ranging from 900 to 1,150 m resulting in a point density of approximately three points/m². The alongshore aircraft trajectory was located above the beach, 0 to 100 m seaward of the seacliff. ALTM elevation points are computed using three sets of data: laser ranges and their associated scan angles, platform position and orientation information, and calibration data and mounting parameters (Wehr and Lohr, 1999). GPS receivers in the aircraft and on the ground at control points provide platform positioning. The GPS receivers record pseudo-range and phase information for post-processing. Platform orientation information comes from an Inertial Measurement Unit (IMU) containing three orthogonal accelerometers and gyroscopes. An aided Inertial Navigation System (INS) solution for the aircraft's attitude is estimated from the IMU output and the GPS information.
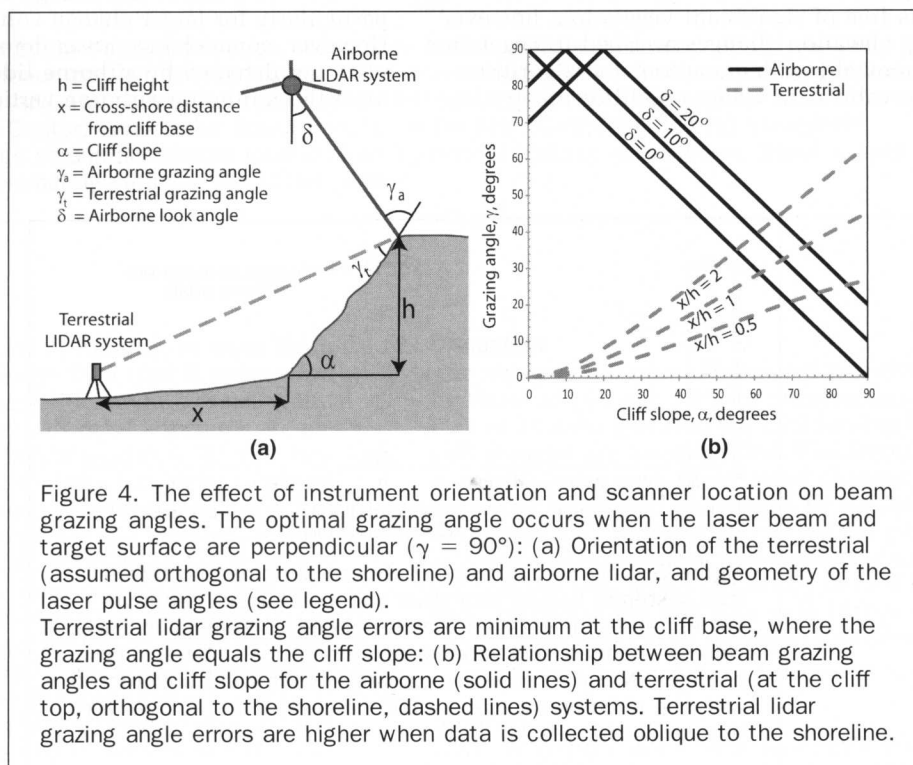
The laser pulse rate of the terrestrial and airborne scanners was 4,400 and 25,000 HZ, respectively. The terrestrial and airborne lidar systems used for this study collected data at about 1 km/hr and 200 km/hr, respectively. The survey cost is generally similar for both methods (approximately $500 to 1,500 USD / km), however a large portion of the coast must be surveyed in order to make airborne data collection economical because of larger mobilization costs. The beam divergence on the terrestrial (2.0 mrad) and airborne (0.2 mrad) scanners resulted in a beam diameter at the target surface ranging from 0.06 to 0.30 m and 0.18 to 0.23 m, respectively (Table 1). The terrestrial lidar system recorded the second pulse of two returns. The airborne system collected two returns, and the second return was used for data processing because it best represents the ground surface.

TABLE 1. TYPICAL SURVEY PARAMETERS FOR THIS STUDY (CLIFF SLOPE, $\alpha = 45°$; CLIFF HEIGHT, $h = 18$ M)

Lidar Sensor	Distance to Cliff Surface (m)	Beam Divergence (mrad)	Beam Diameter at Target Surface (m)	Grazing Angle
Terrestrial	70	2.0	0.14	24–45°
Airborne	1,000	0.2	0.20	45–51°

The terrestrial and airborne point datasets were constructed into digital elevation models using a "natural neighbors" interpolation from a vertical perspective with a grid resolution of 0.2 m, and 0.5 m, respectively. Elevation change maps, the difference between successive surveys, have errors associated with the basic lidar observations (i.e., beam divergence and grazing, georegistration, etc.), as well as from spatial interpolation, and vegetation. The vertical root mean square difference between two surveys (RMS$_Z$; Federal Geographic Data Committee (1998)), a measure of the total error, was estimated using representative fixed sloped surfaces. For the terrestrial surface change maps, RMS$_Z$ = 0.08 m based on repeat surveys of the Del Mar study area on two consecutive days. For airborne lidar change maps, RMS$_Z$ = 0.19 m using concrete covered slopes and a stabilized, partially vegetated slope adjacent to the study area.

Both survey methods have errors arising from beam grazing. Beam grazing related errors depend on the cliff geometry and the position of the scanner relative to the cliff (Figure 4). Errors are maximum (minimum) when the laser beam is parallel (perpendicular) to the target surface (grazing angle $\gamma = 0°$ (90°)). As the slope of an idealized, planar cliff increases, grazing errors increase (decrease) for the airborne (terrestrial) system (Figure 4). With terrestrial

Figure 4. The effect of instrument orientation and scanner location on beam grazing angles. The optimal grazing angle occurs when the laser beam and target surface are perpendicular ($\gamma = 90°$): (a) Orientation of the terrestrial (assumed orthogonal to the shoreline) and airborne lidar, and geometry of the laser pulse angles (see legend).
Terrestrial lidar grazing angle errors are minimum at the cliff base, where the grazing angle equals the cliff slope: (b) Relationship between beam grazing angles and cliff slope for the airborne (solid lines) and terrestrial (at the cliff top, orthogonal to the shoreline, dashed lines) systems. Terrestrial lidar grazing angle errors are higher when data is collected oblique to the shoreline.

lidar, grazing angle errors are maximum at the cliff top (if the cliff does not have overhangs), and narrower beaches and larger cliff heights increase the grazing angle errors. The actual terrain is complex and probably encompasses a full range of slopes at some localized positions on the cliff face.

With the Del Mar average cliff height (18 m) and slope (45°), and typical platform position with respect to the cliff (Table 1), typical terrestrial lidar grazing angles (24° to 45°, data collected orthogonal to the shoreline) are smaller than airborne angles (45° to 51°). Although beam grazing errors are potentially more severe with terrestrial than airborne lidar, the terrestrial lidar was more accurate owing to shorter instrument to surface distance, and a stable platform.

The elevation change grids were filtered and edited to remove noise and erroneous data. First, all grid cells with a vertical change of less than twice the RMS_Z error (terrestrial: 0.16 m, and airborne: 0.38 m) were removed to provide a 95 percent confidence level of change (Federal Geographic Data Committee, 1998). Next, a minimum topographic footprint was imposed, requiring at least ten connected cells of positive or negative change, thus enforcing a minimum change area of 0.4 m², and 2.5 m² for the terrestrial and airborne grids, respectively. These filters result in the detection of individual landslides and talus deposits with a minimum threshold volume of about 0.06 m³ (terrestrial) and 0.95 m³ (airborne) if all ten cells had the minimum change. In practice, the minimum detected volume was approximately double the threshold volume minimums because none of the detected change areas were comprised of all grid cells at both the minimum footprint and elevation thresholds. In some cases, the identified change areas may represent a combination of multiple changes that occurred at the same location during the study period (for example, successive landslides at a single location). Threshold filtering eliminates some valid change, biasing volume estimates away from low values, but significantly improves the confidence of the detected change. The vast majority of the cliff face in the study area was free of significant vegetation, however after grid filtering, elevation changes ascribed to vegetation were manually removed (available automated algorithms sometimes remove valid data where seacliff geometry is complex). Lastly, to evaluate the alongshore variation of cliff change, the 400 m long study area was subdivided into 1 m wide compartments.

Results

In total, the terrestrial lidar detected 112 eroded footprint areas and 70 talus deposits, compared to 25 eroded areas and 20 talus deposits detected by the airborne lidar. The terrestrial lidar detected all individual change areas detected with the airborne lidar and many small changes below the threshold of the aerial system. The difference between the corresponding change area volumes detected by each method ranged from 1 to 100 percent (Figure 5). In general, as the change volume increased, the difference in volume between the two methods decreased. For example, the difference for relatively small (<3 m³, 4 percent of the total change volume), medium (3 to 50 m³, 35 percent of the total change volume), and large (>50 m³, 61 percent of the total change volume) volume changes was 70 percent, 24 percent, and 5 percent, respectively. The airborne erosion volumes were generally less than the terrestrial volumes, except for a few low volume change areas; while the depositional volumes were similar. The terrestrial lidar detected 765 m³ of erosion and 740 m³ of deposition, while the airborne lidar detected 31 percent less erosion (530 m³), and a similar volume of deposition (730 m³, i.e., 1 percent difference).

The volumetric change rate (based on 1 m wide alongshore compartments) ranged between −16 to 12 m³/m, and terrestrial and airborne estimates were highly correlated ($r^2 = 0.95$) (Plate 1). All changes greater than 3 m³/m are spatially coincident between the terrestrial and airborne lidar datasets. Similar to the detected volume data, as the magnitude of alongshore change increases, the correlation usually improves. Deviations occur mostly where large, shallow landslides were below the vertical threshold filter of the airborne lidar (e.g., at location ~325; Plate 1).

The footprint of the change areas generally agreed well, particularly for larger change volumes (Plate 2, Area A). However, some change areas detected by terrestrial lidar were not detected by airborne lidar. These areas did not meet the minimum airborne vertical change (Plate 2, Area
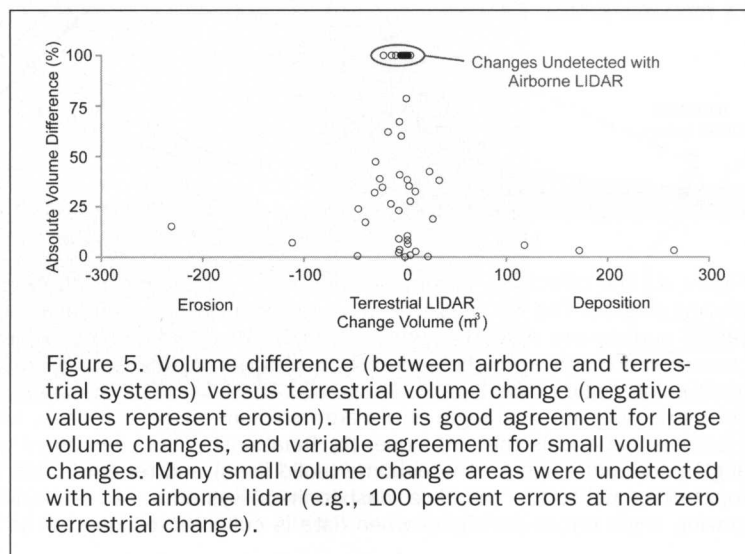

Figure 5. Volume difference (between airborne and terrestrial systems) versus terrestrial volume change (negative values represent erosion). There is good agreement for large volume changes, and variable agreement for small volume changes. Many small volume change areas were undetected with the airborne lidar (e.g., 100 percent errors at near zero terrestrial change).
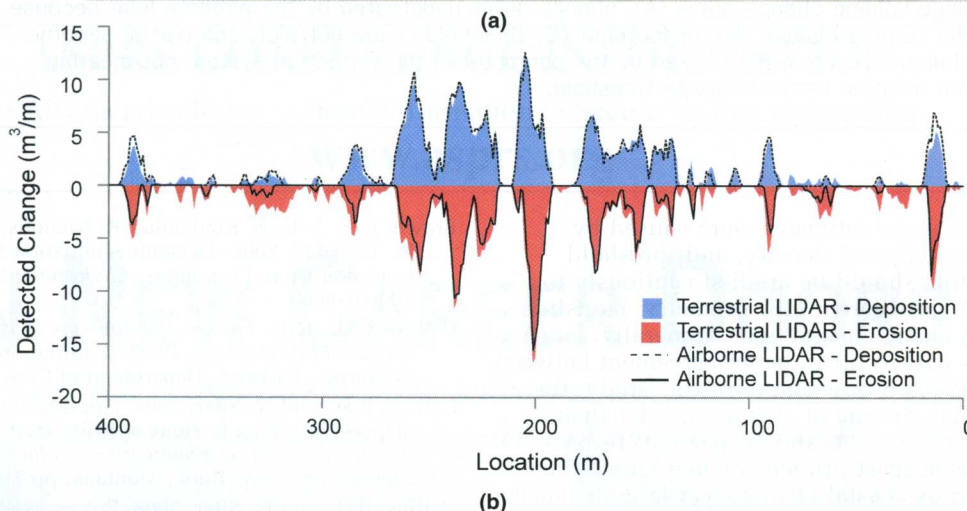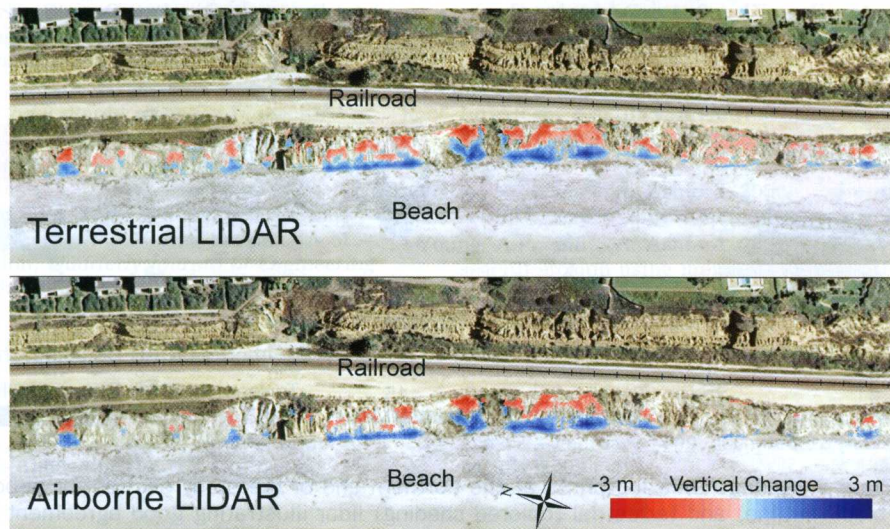
Plate 1. (a) Vertical elevation changes on the seacliff located between the railroad and beach derived from terrestrial and airborne lidar surveys conducted in September 2004 and April 2005 displayed over an orthophotograph (U.S. Geological Survey, EROS Data Center, Sioux Falls, South Dakota) in Del Mar, California, and (b) Volumetric change versus alongshore location from terrestrial (colors) and airborne (black curves approximately outlining the colors) lidar.
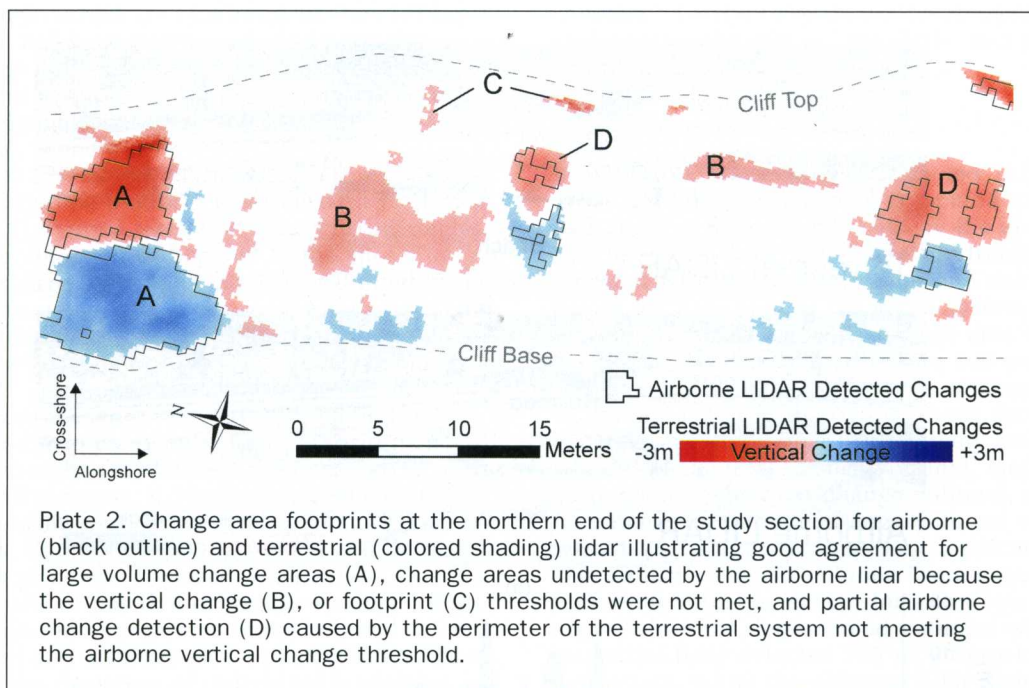
B), footprint threshold (Plate 2, Area C), or were limited by the airborne lidar accuracy. Two type B areas were relatively large, shallow landslides with a mean vertical change of 0.31 m (volume = 13 m^3, footprint = 42 m^2), and 0.26 m (volume = 21 m^3, footprint = 79 m^2). In some cases, cells on the perimeter of the terrestrial detected change did not meet the vertical airborne threshold resulting in smaller airborne footprints and smaller change volumes (Plate 2, Area D). In addition to the threshold requirements, the airborne lidar surface change was systematically positively biased (0.02 m, estimated on the cliff top), which contributed to differences in the detected footprint and change volumes. The terrestrial change grid (e.g., Plate 2), resampled to the resolution (0.5 m by 0.5 m) and cell alignment of the airborne change grid using a bilinear interpolation, was highly correlated with the airborne grid (r^2 = 0.90).

Discussion

The airborne lidar underestimated negative change (erosion) by about 30 percent, perhaps because thin layers (less than 0.38 m as measured into the cliff face) of broadly eroded cliff material are not measured. The largest slides were most accurately measured. Many small changes detected by the terrestrial lidar were undetected by the airborne lidar. On the other hand, airborne and terrestrial estimates of total positive change volumes (deposition) agreed well, perhaps because the thin layers of broadly eroded cliff material were concentrated at the cliff base with higher elevation change values, thus permitting increased detection by airborne lidar.

Summary

This study provides a basic comparison of airborne and terrestrial lidar measurements of seacliff change.

Plate 2. Change area footprints at the northern end of the study section for airborne (black outline) and terrestrial (colored shading) lidar illustrating good agreement for large volume change areas (A), change areas undetected by the airborne lidar because the vertical change (B), or footprint (C) thresholds were not met, and partial airborne change detection (D) caused by the perimeter of the terrestrial system not meeting the airborne vertical change threshold.

Differences in cliff change estimates were caused by differences in accuracy, point density, and threshold filtering. These results should be applied cautiously to other areas with much different cliff geometry, landslide characteristics, and change magnitudes. Generally, larger magnitude changes will result in better agreement between the two survey methods. For example in this study, the difference in the total volume of changes greater than, and less 3 m³, was 12 percent, and 70 percent, respectively. These results suggest prudence when employing airborne lidar to assess coastal change over long distances (for sediment budget or erosion rate purposes) if relatively small volume changes constitute a significant amount of eroded material.

References
Adams, J.C., and J.H. Chandler, 2002. Evaluation of LIDAR and medium scale photogrammetry for detecting soft-cliff coastal change, *The Photogrammetric Record*, 17(99):405–418.

Böhm, J., and N. Haala, 2005. Efficient integration of aerial and terrestrial laser data for virtual city modeling using lasermaps, *Proceedings of the ISPRS Workshop on Laser Scanning*, International Archives of Photogrammetry and Remote Sensing, Vol. 36 Part 3/W19, 192–197.

Benumof, B.T., and G.B. Griggs, 1999. The dependence of seacliff erosion rates, cliff material properties, and physical processes: Sand Diego County, California, *Shore & Beach*, 67(4):29–41.

Brown, I., S. Jude, S. Koukoulas, R. Nicholls, M. Dickson, and M. Walkden, 2006. Dynamic simulation and visualization of coastal erosion, *Computers, Environments and Urban Systems*, 30:840–860.

Collins, B.D., 2004. *Failure Mechanisms of Weakly Lithified Sand Coastal Bluff Deposits*, Ph.D. Dissertation, University of California, Berkeley, Department of Civil Engineering, 278 p.

Collins, B.D., and N. Sitar, 2004. Application of high resolution 3D laser scanning to slope stability studies, *Proceedings of the 39th Symposium on Engineering Geology and Geotechnical Engineering*, May, Butte, Montana, pp 79–82.

Collins, B.D., and N. Sitar, 2008. Processes of coastal bluff erosion in weakly lithified sands, Pacifica, California, *Geomorphology*, 97:483–501.

Federal Geographic Data Committee, 1998. *Geospatial Positioning Accuracy Standards*, FGDC-STD-007.3-1998, 28 p.

Hapke, C.J., and D. Reid, 2007. *National Assessment of Shoreline Change, Part 4: Historical Coastal Cliff Retreat along the California Coast*, U.S. Geological Survey Open-file Report 2007–1133, 51 p.

Iavarone, A., and D. Vagners, 2003. Sensor fusion: generating 3D by combining airborne and tripod mounted lidar data, *International Archives of Photogrammetry, Remote Sensing and Spatial information Sciences*, Vol. XXXIV-5W10.

Kennedy, M.P., 1975. *Geology of the San Diego Metropolitan Area, Western Area*, California Division of Mines and Geology Bulletin 200, 56 p.

Kuhn, G.G., and F.P. Shepard, 1984. *Sea Cliffs, Beaches, and Coastal Valleys of San Diego County: Some Amazing Histories and Some Horrifying Implications*, Berkeley, California, University of California Press, 193 p.

Leyland, J., and S.E. Darby, 2008. An empirical-conceptual gully evolution model for channeled sea cliffs, *Geomorphology*, 102:419–434.

Lim, M., D.N. Petley, N.J. Rosser, R.J. Allison, and A.J. Long, 2005. Combined digital photogrammetry and time-of-flight laser scanning for monitoring cliff evolution, *The Photogrammetric Record*, 20(110):109–129.

Miller, P., J. Mills, S. Edwards, P. Bryan, S. Marsh, P. Hobbs, and H. Mitchell, 2007. A robust surface matching technique for integrated monitoring of coastal geohazards, *Marine Geodesy*, 30:109–123.

Moore, L.J., B.T. Benumof, and G.B. Griggs, 1999. Coastal erosion hazards in Santa Cruz and San Diego Counties, California, Coastal Erosion Mapping and Management, *Journal of Coastal Research* (M. Crowell and S.P. Leatherman, editors), SI 28:121–139.

Olsen, M.J., E. Johnstone, S.A. Ashford, N. Driscoll, A.P. Young, T.J. Hsieh, and F. Kuester, 2008. Rapid response to seacliff erosion in San Diego County, California using terrestrial LIDAR, *Proceedings of the ASCE Solutions to Coastal Disasters 2008*, Oahu, Hawaii, 573–583.

Rosser, N.J., D.N. Petley, M. Lim, S.A. Dunning, and R.J. Allison, 2005. Terrestrial laser scanning for monitoring the process of hard rock coastal cliff erosion, *Quarterly Journal of Engineering Geology and Hydrology*, 38:363–375.

Sallenger, Jr., A.H., W. Krabill, J. Brock, R. Swift, S. Manizade, and H. Stockdon, 2002. Sea-cliff erosion as a function of beach changes and extreme wave runup during the 1997–1998 El Niño, *Marine Geology*, 187:279–297.

Wehr, A., and U. Lohr, 1999. Airborne laser scanning - An introduction and overview, *ISPRS Journal of Photogrammetry and Remote Sensing*, 54 (2–3):68–82.

Young, A.P., 2006. *Quantifying Short-Term Seacliff Morphology of a Developed Coast: San Diego County, California*, Ph.D. Dissertation, University of California San Diego, Jacobs School of Engineering, 208 p.

Young, A.P., and S.A. Ashford, 2006a. Application of airborne LIDAR for seacliff volumetric change and beach-sediment budget contributions, *Journal of Coastal Research*, 22(2):307–318.

Young, A.P., and S.A. Ashford, 2006b. Performance evaluation of seacliff erosion control methods, *Shore & Beach*, 74:16–24.

Young, A.P., and S.A. Ashford, 2007. Quantifying sub-regional seacliff erosion using mobile terrestrial LIDAR, *Shore & Beach*, 75:38–43.

Young, A.P., and S.A. Ashford, 2008. Instability investigation of cantilevered seacliffs, *Earth Surface Processes and Landforms*, 33:1661–1677.